Design and construction of a pyramidal Magneto-Optical Trap for laser cooling of rubidium atoms

Master's thesis
by
Stefan Magnusson

Lund Reports on Atomic Physics, LRAP-339
Lund, March 2005

Dedicated to my Father,
whose decease has affected me in many ways

Abstract

In this Master's thesis a pyramidal Magneto-Optical trap (MOT) for rubidium has been designed and constructed. This will be used in the Atomic physics cources for undergraduate students at Lund Technical University.

The theory for Laser Cooling and Trapping is covered. A detailed instruction of how to design and build a low-cost MOT is presented.

All necessary components are now in the picosecond laboratory of Lund High Power Laser Facility.

This report is a continuation of another Master's thesis, Lund Reports on Atomic Physics (LRAP) 325.

Contents

Chapter 1

Introduction

When atoms or molecules interact with light by absorption, spontaneous or stimulated emission, important information about their physical properties emerges. This is the foundation for all spectroscopy. Atoms or molecules can also be manipulated by the light, e.g. their velocity and spatial distribution can be changed. This is called *Laser Cooling*.

1.1 Research

Laser Cooling is the biggest area of research in Atomic Physics today. Unfortunately, the only group in Sweden performing this kind of research is Anders Kastberg's group in Umeå. Our hope is that Lund soon will offer students training in Laser Cooling on an undergraduate level.

During the last two decades laser cooling has seen a fantastic development, including two Nobel prizes 1997[1] and 2001[2]. Now it is standard to cool samples of neutral atoms down to microns of a Kelvin and keep them in a confined space for seconds allowing researchers to control atomic motion in a whole new way. It's not hard to understand why this is very useful for atomic research.

The most famous application is the Bose-Einstein Condensate (BEC), that gave the Nobel Prize in 2001. This happens when atoms get so cold and confined so that they will all condensate into the lowest possible energy level.

Another recent application, is the use of a MOT to do ^{81}Kr dating. This allows scientists to date objects much earlier than the 50 000 year limit of ^{14}C dating (up to 230 000 years) [35].

[1] S. Chu, C. Cohen-Tannoudji and W.D. Phillips [22].
[2] E.A. Cornell, W. Ketterle and C.E. Wieman [23].

1.2 The project

The aim of this thesis was to build a Magneto-Optical Trap (MOT) for modern state-of-the-art laboratory exercises. Erik Gustavsson [1] started the project one year ago by building the two external cavity diode lasers and doing some initial design studies. My task was to finish the design and to purchase and build the necessary equipment.

The two most challenging aspects of the project were the very low budget and lack of cometence in house. However, the reward is big, since laser cooling and trapping of neutral atoms is very suitable for undergraduate educational purposes. The physics behind is exciting and easy understandable with atomic physics background. There are a lot of experimental skills involved; laser operation, optical alignment, lock-in amplification, regulator systems and vacuum systems. It can also be performed with small resources.

1.3 Outline

Chapter 2 gives a theoretical background to laser cooling. Some of the theory covered is outlined as an instruction with preparatory exercises and solutions to use in the future laboratory exercise instructions.

Chapter 3 describes the experimental setup of the MOT, including the vacuum chamber, the Rb-source, the pyramidal mirror, the observation system, the magnetic field and the system for release and recapture.

Chapter 4 describes the optical setup, including the lasers and the saturation spectroscopy setup.

Chapter 2

Cooling and trapping of Rubidium

The aim of this thesis is to build a MOT for undergraduate educational purposes. Some of the theory covered are outlined as an instruction with preparatory exercises and solutions to use in future laboratory experiment instructions.

2.1 Rubidium, an Alkali-metal

Rubidium is an Alkali-metal. The Alkali-metals were the first group of atoms that was cooled and trapped [36]. They have transitions from the ground state to the excited states, that correspond to wavelengths in the visible or the near infrared (NIR) regions. They can also easily be generated in atomic beams. These two properties make them very suitable for cold atom experiments. Natural rubidium contains two isotopes ^{85}Rb (72 %) and ^{87}Rb (28 %), but in this thesis we only consider the isotope ^{87}Rb.

The level scheme for ^{87}Rb is found in figure 2.1 and some data in table 2.1.

2.2 Cooling...

If a bowling ball is moving towards you and you are throwing table tennis balls at it, it will eventually come to a stop. You will need a lot of table tennis balls but the momentum transfer at each hit will slow the bowling ball down and even change the direction. The concept of laser cooling is similar.

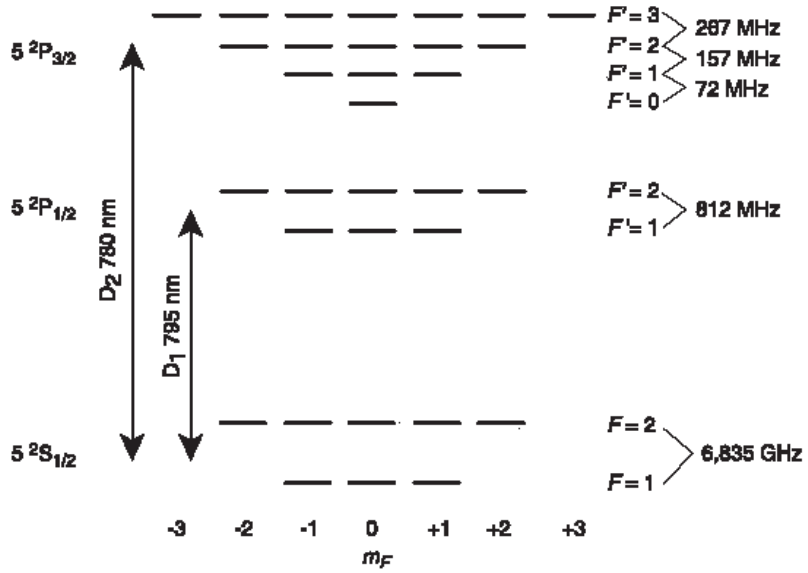

Figure 2.1: Level scheme of ^{87}Rb with nuclear spin $I = 3/2$.[12]

Nuclear spin I	3/2
Mass	86,9902 u [7]
g-Factor g_I	-0.0009951414 [12]
Vacuum wavelength D1-transition	794.979 nm [7]
Vacuum wavelength D2-transition	780.241 nm [7]
Line width D1-transition γ_{D1}	5.58 MHz [7]
Line width D2-transition γ_{D2}	6.01 MHz [7]
Life time $5^2P_{1/2}$	28.5 ns [7]
Life time $5^2P_{3/2}$	26.5 ns [7]
Saturation intensity I_s	1.654 mW/cm^2 [7]
Ground state hyperfine splitting	6834682612.8 Hz [8]

Table 2.1: Some physical properties of ^{87}Rb, more can be found in [9].

2.2.1 Light force

The momentum kick that each atom receives when absorbing a photon is very small, the velocity change is in the region of 1 cm/s[1]. However, because of the very high intensity of the laser light a huge number of photons hit the atom every second. In thesis the D2-line in rubidium-87, that is the transition $5s^2S_{1/2}(F=2) \rightarrow 5p^2P_{3/2}(F=3)$, provides a good possibility for cooling. First it is a closed transition[2] (figure 2.2) where the excited atom only can deexcite to the same level. Secondly it is quite easy to find diodes that lase around 780 nm where the transition lies.

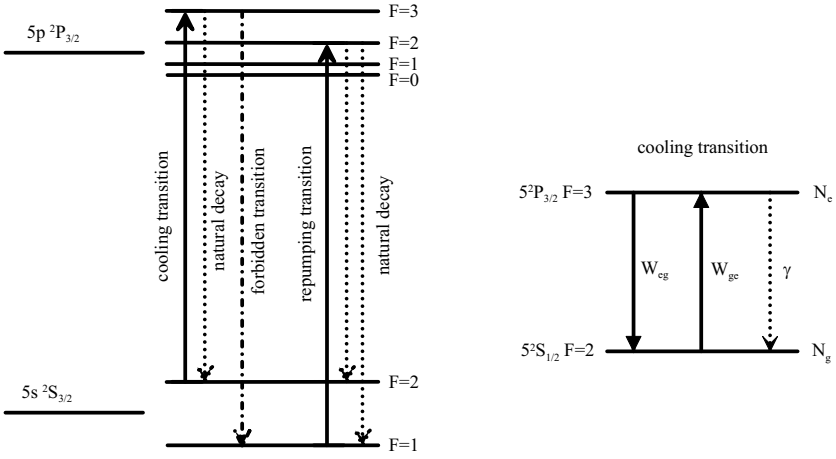

Figure 2.2: *Left:* The transitions in ^{87}Rb used in laser cooling. *Right:* Two-level scheme of the cooling transition.

Preparatory exercise 1 *Write down the rate equation to describe the populations N_g and N_e due to absorption (W_{ge}), stimulated (W_{eg}) and spontaneous emission (γ). Find the stationary solution and calculate $N_e(N_{tot}, W, \gamma)$, where $N_{tot} = N_e + N_g$ and $W_{eg} = W_{ge} = W$ (see figure 2.2 right).*

Solution exercise 1 *The rate equations are*

$$\frac{dN_g}{dt} = \gamma N_e + W_{eg}N_e - W_{ge}N_g$$

$$\frac{dN_e}{dt} = -\gamma N_e - W_{eg}N_e + W_{ge}N_g$$

[1] This is actually the same order of magnitude as the velocity change that a bowling ball experiences when table tennis balls are thrown at it.

[2] Closed in the sense that the atoms have to perform a forbidden transition to leave these two transitions.

A steady state solution of the rate equations gives the fraction of excited atoms, $N_{tot} = N_e + N_g$ *and* $W_{eg} = W_{ge} = W$*:*

$$N_e(N_{tot}, W, \gamma) = N_{tot} \frac{W/\gamma}{1 + 2W/\gamma} \tag{2.1}$$

To be able to cool the atoms one must select only the fast moving atoms, the ones that are still should not be affected. The Doppler effect works to our advantage. If the laser is detuned to red of the cooling transition, the fast moving atoms will see the laser light at a higher frequency and closer to transition (figure 2.3).

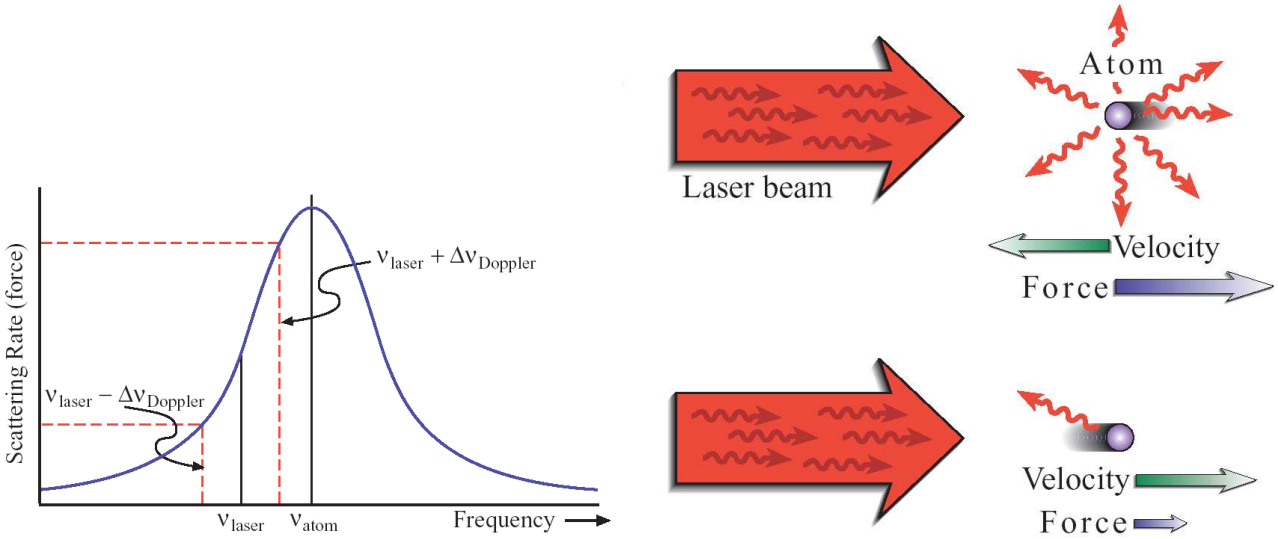

Figure 2.3: *Left:* Atomic scattering rate versus laser frequency. *Right:* Laser detuned to the red of atomic resonance. Due to Doppler shift, atoms moving towards the laser beam will scatter photons at a higher rate which leads to a cooling force proportional to the velocity. [34]

The absorption rate W can be expressed as

$$W = \frac{I}{h \cdot \omega} \cdot \sigma(\nu)$$

where ω is the laser frequency and the absorption cross section σ is written as [36]

$$\sigma(\nu) = \frac{\sigma_0}{1 + (2\delta/\gamma)^2}$$

where σ_0 is the cross section at the resonance frequency, δ the laser detuning and γ the natural line width [rad/s] [2]. $\delta = \nu - \nu_{eg}$ where ν is the laser frequency and ν_{eg} the resonance frequency.

Preparatory exercise 2 *Insert the expressions above in the result that you obtained from exercise 1 and simplify the expression using the saturation intensity* $I_s = \frac{h\nu\gamma}{2\sigma_0}$.

Solution exercise 2 *Using equation 2.1 and inserting the expressions above yields:*

$$N_e = N_{tot}\frac{1}{2}\frac{I/I_s}{1+(2\delta/\gamma)^2+I/I_s} \tag{2.2}$$

Preparatory exercise 3 *Use the* N_e *that you calculated in exercise 2 to calculate the scattering rate* $R(I, I_s, \delta, \gamma) = (N_e/N_{tot}) \cdot \gamma$

Solution exercise 3 *The scattering rate can be expressed as*

$$R(I, I_s, \delta, \gamma) = N_e/N_{tot} \cdot \gamma = \frac{1}{2}\ \frac{\gamma \cdot I/I_s}{1+(2\delta/\gamma)^2+I/I_s} \tag{2.3}$$

The cooling force equals the scattering rate times the momentum transfer. The momentum kicks from the photons, originating from spontaneous emission, are neglected since they act in random directions and do not contribute to the average force.

$$\vec{F} = R\vec{p} = \frac{1}{2}\frac{I/I_s}{1+(2\delta/\gamma)^2+I/I_s}\gamma\hbar\vec{k} \tag{2.4}$$

An atom with a velocity $\vec{v}$ "sees" a higher frequency than the laser frequency, displaced by the Doppler shift:

$$\delta_d = -\vec{k}\cdot\vec{v}$$

where $\vec{k}$ is the wave vector of the laser beam. For two counter-propagating beams with wave vectors $\vec{k}$ and $-\vec{k}$ the cooling force in the overlap region is

$$\begin{aligned}\vec{F} = \frac{1}{2}\Bigg[&\frac{I/I_s}{1+\left(2\frac{\delta-\vec{k}\cdot\vec{v}}{\gamma}\right)^2+I/I_s} \\ &-\frac{I/I_s}{1+\left(2\frac{\delta+\vec{k}\cdot\vec{v}}{\gamma}\right)^2+I/I_s}\Bigg]\gamma\hbar\vec{k}\end{aligned} \tag{2.5}$$

The cooling force on ^{87}Rb is plotted for various detunings in figure 2.4.

Preparatory exercise 4 *Use a Taylor expansion of equation 2.5 to show that F is a* friction force *($\vec{F}(\vec{v}) = -b\cdot\vec{v}$) for small v (compare with figure 2.4). Give an expression for b.*

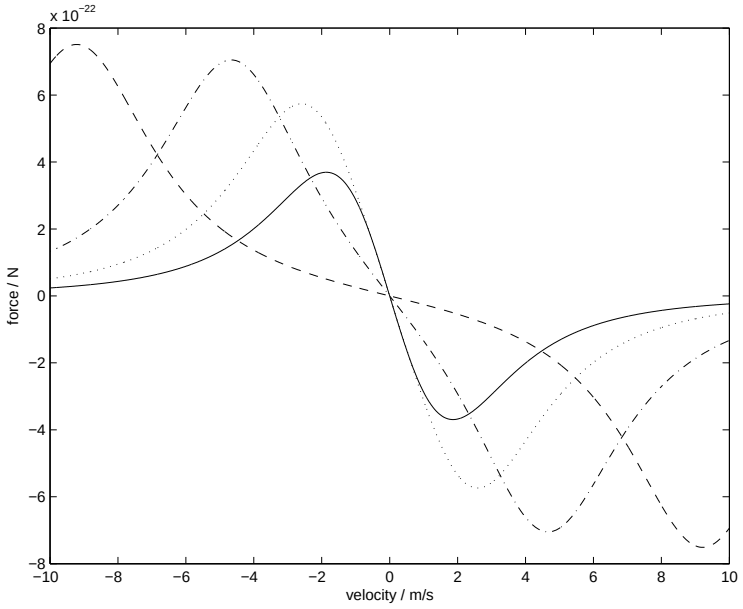

Figure 2.4: The friction force on ^{87}Rb for various detunings as a function of velocity. The beam is assumed to have I=10 mW/cm^2 ($I_s = 1.6$ mW/cm^2, $\gamma = 5.9$ MHz). Laser detuning $\delta = -\frac{\gamma}{4}$, solid line; $\delta = -\frac{\gamma}{2}$, dotted line; $\delta = -\gamma$, dash-dotted line and $\delta = -2\gamma$, dashed line.[1]

Solution exercise 4 *We find:*

$$\vec{F}(\vec{v}) = -b\vec{v}$$

with

$$b = -\frac{8(I/I_s)k^2\delta\hbar}{\gamma(1 + (2\delta/\gamma)^2 + (I/I_s))^2}$$

This gives that $\vec{F}(\vec{v})$ is a cooling force if $\delta < 0$, i.e. detuned to the "red" of the transition.

The results above can be generalized to three dimensions, giving rise to *Optical Molasses* that was the predecessor of the MOT (see figure 2.5).

2.2.2 Hyperfine pumping

Unfortunately the Rb does not have a totally closed two-level scheme. In about 1/1000 of the deexcitations there is a forbidden transition [4]. The atoms end up in the $F = 1$ state and can no longer be cooled. There is a need for a second laser that can repump the atoms to the excited state $F = 2, 3$. This laser can be much weaker and less precise in frequency than the cooling laser.

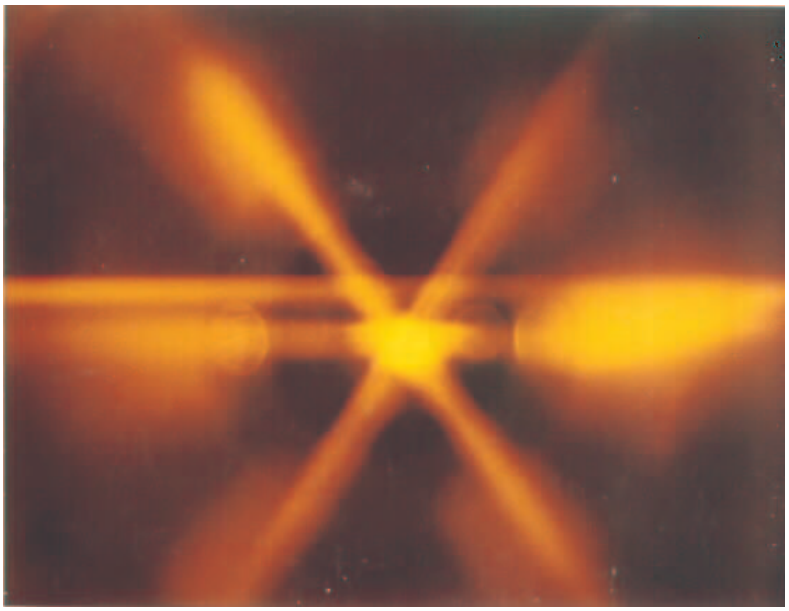

Figure 2.5: An optical molasse of neutral sodium.[10]

2.2.3 Doppler limit

The cooling procedure, also called Doppler cooling for obvious reasons, leads to a temperature whose lower limit lies in the order of $\hbar/\tau$ where $\tau = \gamma^{-1}$ is the lifetime of the excited state [20].

The cooling force leads to a loss of kinetic energy

$$(dE/dt)_{cool} = Fv = -bv^2 = \frac{8(I/I_s)k^2\delta\hbar}{\gamma(1+(2\delta/\gamma)^2)^2}v^2 \tag{2.6}$$

where F is the friction force in equation 2.5 along some arbitrary axis and b was derived in exercise 4 (using that $I \ll I_s$). This damping force reduces the average velocity of the atom towards zero, but the mean squared velocity does not go to zero. While the cooling process removes kinetic energy, the heating from the randomness of absorption and emission of photons increases it. The heating can be compared to a random walk in one dimension and we have

$$d(p^2)/dt = 2\hbar^2k^2R.$$

This gives the change in kinetic energy ($E = p^2/2M$)

$$(dE/dt)_{heat} = \hbar^2k^2R/M = \frac{\hbar^2k^2\gamma}{M}\frac{I/I_s}{1+(2\delta/\gamma)^2} \tag{2.7}$$

where the scattering rate is twice that[3] derived in section 2.2.1 and the

[3] Due to the two counter-propagating beams.

approximations [29] $|kv| \ll |\delta|$, $|kv| \ll \gamma$ (since v is small) and $I \ll I_s$ are used.

The result at equilibrium ($(dE/dt)_{cool} + (dE/dt)_{heat} = 0$, solving for v^2) is

$$v^2 = \frac{\hbar\gamma}{4M} \frac{1 + (2\delta/\gamma)^2}{2|\delta|/\gamma} \tag{2.8}$$

The thermal energy is $k_B T/2$ per degree of freedom, so in our one-dimensional example we have

$$M\langle v^2 \rangle/2 = k_B T/2 \Rightarrow k_B T = \frac{\hbar\gamma}{4} \frac{1 + (2\delta/\gamma)^2}{2|\delta|/\gamma} \tag{2.9}$$

The expression above is valid in 3-D if $\hbar^2 k^2/2M \ll \hbar\gamma$ [22]. The cooling rate is proportional to the kinetic energy and by contrast the heating is proportional to the photon scattering rate, independent of atomic kinetic energy for low velocities.

Minimizing equation 2.9 gives the so called Doppler cooling limit, first derived by Letokhov, Minogin and Pavilik [20]:

$$k_B T_D = \frac{\hbar\gamma}{2} \tag{2.10}$$

occurring when $\delta = -\gamma/2$, which for Rb gives $T_D = 140\ \mu$K.

2.2.4 Subdoppler cooling

In 1988 Lett's group published that they surprisingly had reached far below the Doppler limit [30]. Two groups found a model that explained this discrepancy [31, 32]. The multiplicity of sublevels (e.g. Zeeman and hyper-fine structure) of the atomic state gives rise to a dynamic close to optical pumping between the levels. If the light-field varies in space, the optical pumping tries to adjust the atomic orientation to the changing field. Since the pumping process is rather weak, it always lag behind the changings of the field leading to a non-adiabatic process that makes further cooling possible. We give two examples of such additional cooling mechanisms below.

Sisyphus cooling

> In the underworld Sisyphus was compelled to roll a big stone up a steep hill; but before it reached the top of the hill the stone always rolled down, and Sisyphus had to begin all over again (Odyssey, xi. 593)... The reason for this punishment is not mentioned in Homer, and is obscure; according to some, he had revealed the designs of the gods to mortals, according to others, he was in the habit of attacking and murdering travelers.[33]

If counter propagating beams are linearly polarized with perpendicular polarization one gets a standing wave pattern with alternating polarization, see figure 2.6.

Just like the underworld Sisyphus, the atoms in motion always experience a potential with positive derivative, hence slowing them down.

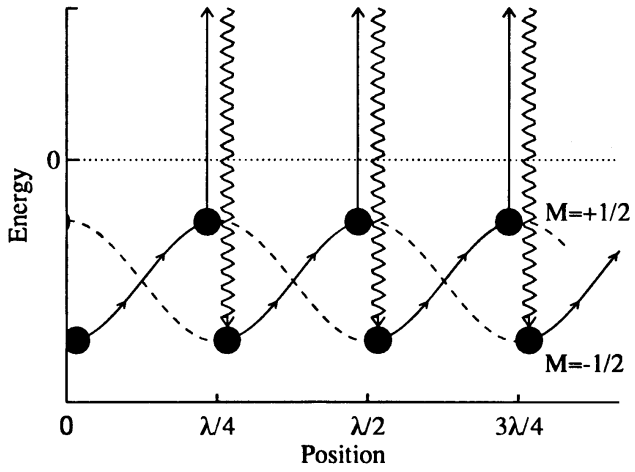

Figure 2.6: The light shift and transitions of Sisyphus cooling.[36]

$\sigma^+ - \sigma^-$ cooling

If the counter propagating beams are circularly polarized with opposite polarization direction, this gives a possibility to cool beyond the Doppler limit as well. The standing wave in this case is a rotating linearly polarized magnetic field that rotates $2\pi/\lambda$. The atoms move slower than the rotating field and can not be pumped quick enough. The atoms that moves against the σ^--beam have a higher probability to end up in the $M_g = -2$ state and there they have a higher probability of absorbing a σ^--photon. The same argument holds for the atoms moving against the σ^+-beam. This leads to an increased damping force.

In our MOT setup there will be polarization effects like this and it is possible (but not likely) to obtain temperatures down to 1 μK [6] which is two orders of magnitude smaller than the Doppler limit.

2.2.5 Recoil limit

The lowest possible temperature for any optical cooling process corresponds to the momentum of a single photon. So far, the recoil of the atom has been

neglected, but for temperatures in the nK range it is a severe problem. This limit is far beyond the goals for this project. For the sake of completeness the recoil limit for Rb is 0.6 cm/s or 0.4 μK.

2.3 ... and Trapping

Even if we have cooled atoms in the section above, they will still diffuse out of the region covered by the lasers if there is not a position dependent force as well. There are many ways to obtain this but in this experiment we will use the most common one, a Magneto-Optical trap (MOT), also known as Zeeman shift optical trap (ZOT). These names gives a brief idea about how it is done. Below we explain the principle of a MOT in one dimension and for a simple $J = 0 \rightarrow J = 1$ two level scheme.

Trapping is achieved by adding to Doppler cooling an inhomogeneous magnetic field, and by a clever choice of the laser polarization as explained in figure 2.7. The magnetic field ($B = B(z)$) will lead to Zeeman splitting of the magnetic sublevels (figure 2.1).

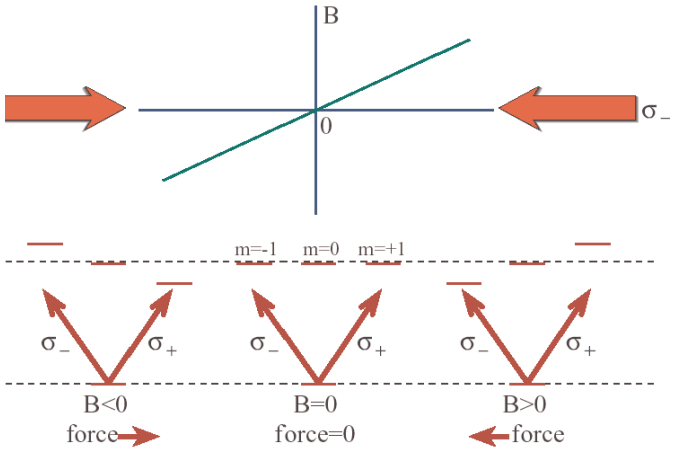

Figure 2.7: Laser beams with opposite circular polarization traveling in the z-direction. The laser beams excite the $J = 0 \rightarrow J = 1$ transition. The laser beam from the right only excites the $m = -1$ state and the laser beam from the left only excites the $m = +1$ state. As an atom moves from right to left, these levels are shifted by the magnetic field, thereby affecting the photon scattering rates. The net result is a position-dependent force that pushes the atom towards the center.[34]

The excited state splits into three sublevels which all have different excitation probabilities depending on the polarization (e.g σ^+ favors the transition $\Delta M_F = 1$). The result is a restoring force as described schematically in figure 2.7, lower part.

The frequency shift for the Zeeman effect can be expressed as

$$\delta_{\pm}(z) = -\frac{g_e \cdot M_e - g_g \cdot M_g}{\hbar}\mu_B \cdot B(z)$$

where g_i and M_i are the g-factor and magnetic quantum number for the different states, δ_+ is the shift for the σ^+ beam, δ_- is the shift for the σ^- beam and μ_B the Bohr magneton.

Preparatory exercise 5 *Calculate the frequency shift due to the Zeeman effect as a function of z in the D2-line of* ^{87}Rb *for a linear magnetic field* $B(z) = A \cdot z$.

Solution exercise 5 $g_g = 1/2$, $g_e = 2/3$, $M_g = \pm 2$ *and* $M_e = \pm 3$ *gives*

$$\delta_{\pm} = \mp\frac{A\mu_B}{\hbar}z$$

Preparatory exercise 6 *Derive an expression for the trapping force.*

Solution exercise 6 *Using equation 2.5 and inserting the solution from exercise 5 one obtain*

$$\vec{F} = \frac{1}{2}\left[\frac{I/I_s}{1 + \left(2\frac{\delta - \vec{k}\cdot\vec{v} + \delta_+}{\gamma}\right)^2 + I/I_s} - \frac{I/I_s}{1 + \left(2\frac{\delta + \vec{k}\cdot\vec{v} + \delta_-}{\gamma}\right)^2 + I/I_s}\right]\gamma\hbar\vec{k}$$

Analogue to exercise 4 one can show[4] that $\vec{F}(z) = -k_H z$ if $\delta < 0$, i.e. $\vec{F}(z)$ is a *trapping force*.

The total force on the atom is a highly over-damped harmonic oscillator potential (after a simple extension to three dimensions):

$$\vec{F}_{atom} = -b\vec{v} - k_H\vec{r}$$

The fact that the trap is a highly over-damped system is very important since the performance of the trap and the lifetime almost entirely depends on the cooling force[5]. However, the number of trapped atoms depends weakly on the cooling parameters but strongly on the trapping force[6]. The theory for calculating these two very important properties of the MOT follows below.

[4] This is quite messy and will not be given as an exercise.

[5] Beam diameter, power and frequency of the laser all strongly affect the lifetime.

[6] Magnetic fields, stray or applied, and laser beam polarization and alignment all strongly affect the number of trapped atoms.

2.3.1 Lifetime

The number of atoms in the trap will increase with the same characteristics as a charging capacitor [36]

$$N(t) = N_0(1 - e^{-t/\tau}) \tag{2.11}$$

where τ is the time constant to fill the trap to the steady-state value N_0. $\tau^{(-1)}$ is just the loss rate from the trap due to collisions with the hot background gas.

2.3.2 Number of trapped atoms

Equation 2.3 gives an expression for the number of photons scattered per atom and second. If one measures the difference in fluorescence with and without the trapping magnetic field with a photodiode (here called Δ_p) the expression for the number of atoms becomes

$$N = \frac{\Delta_p}{RE_{photon}} \tag{2.12}$$

Preparatory exercise 7 *Two important corrections have to be done to equation 2.12 to make it useful in the lab. Which?*

Solution exercise 7 *The efficiency of the photodiode and the solid angle has to be accounted for:* $N = \Delta_p/(\eta_{photodiode} RE_{photon} \Omega)$.

2.4 Measurement of Temperature

The classical, thermodynamic, interpretation of the dimensionless constant that we normally call temperature, origin back to Lord Kelvin. The calculation can be found in any textbook in thermodynamics (e.g. [21]). The foundation of the theory is ideal gases in equilibrium but the environment of the MOT with extremely low temperature and pressure are far from this idealization, hence the thermodynamic treatment makes no sense. Although the laser-cooled cloud of atoms can in no way be in thermodynamic equilibrium (the velocity of the atoms is in the order of cm/s), they can still be in a steady-state situation and have a Gaussian distribution [26, 27][7] and we can define a "temperature" from the width of the velocity distribution.

[7] The solution of the Fokker-Plank equation for a system acted on by a force proportional to velocity with a random input not dependent on velocity, is a Maxwell-Boltzmann distribution.

2.4.1 Release and recapture

One way to measure the temperature is the so called release and recapture method. First performed in 1985 by Phillips [24] and Chu [25], it provides a simple way to determine the width of the velocity distribution with a ballistical technique. The MOT is loaded and the cooling laser and the trapping field are turned off simultaneously. Since the magnetic field originates from coils, there are a slight lag between the shut-off and when the field reaches zero. This time is less than 500 μs [15] and therefore negligible in this application.

After a period of time (release time), the lasers and the magnetic field are turned back on. For 50 ms the MOT captures the atoms again (recapture time). Since this time is much less than the filling time of the MOT, the capture from the background vapor is negligible. The fluorescence is measured before the release and after the capture. Atoms with high temperature have time to leave the capture region and the number of recaptured atoms decays fast with the release time. The R&R data for different release times are fitted to a theoretical Maxwell-Boltzmann velocity distribution where the spatial distribution (Gaussian) and the gravitational pull have been taken into account. Two measurements by Shih-Kuang Tung [15] with R&R can be found in figure 2.8.

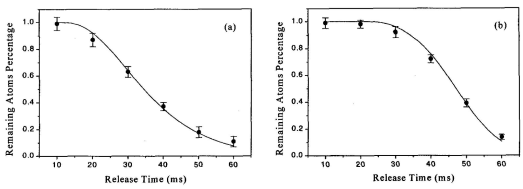

Figure 2.8: (a) and (b) are the R&R measurements, where circular points are the experimental data and solid curves are the results of the theoretical calculation. The theoretical curves correspond to 320±40 μK in (a) and 80±10 μK in (b). The temperature uncertainties include the errors due to the fitting and the fluctuations between experimental runs.[15]

Chapter 3

The MOT

Here, we describe the different components of the constructed MOT: the vacuum chamber, the Rb-source, the observation system, the pyramidal mirror, the magnetic field and the system for release and recapture. A scheme of the entire setup with the electronical couplings can be seen in figure 3.1.

3.1 Vacuum chamber

The vacuum system has to pump down to a pressure of typically a few 10^{-9}mbar (or 10^{-7}Pa). Although a MOT at a pressure of 10^{-8}mbar has been reported [6], a lower pressure gives better conditions (e.g. longer lifetime) for trapping and cooling atoms.

The chamber is built of standard ConFlat parts to reach the lowest possible pressure. A three-way cross is mounted on top with a window and an electrical feedthrough. Another three-way cross is mounted underneath with a low pressure gauge and an adapter to a molecular pump. All is mounted on a table designed by the author and manufactured at the academic workshop. For a sketch and photo of the chamber, see figure 3.2.

3.1.1 Assembly

The ConFlat flange assembly consists of two knife edges that are pressed into a copper gasket. The flanges are cleaned first by a strong cleaning agent, then with pure methanol. After cleaning and wipe-off, the vacuum parts are only touched with clean latex gloves. The copper gasket should only be touched with gloves as well. The gaskets are one-time usage and a fresh gasket should always be used. The bolts are then tightened in a criss-cross pattern until the assembly is tight. For a more detailed discussion of cleaning and assembly, see [16] and [17].

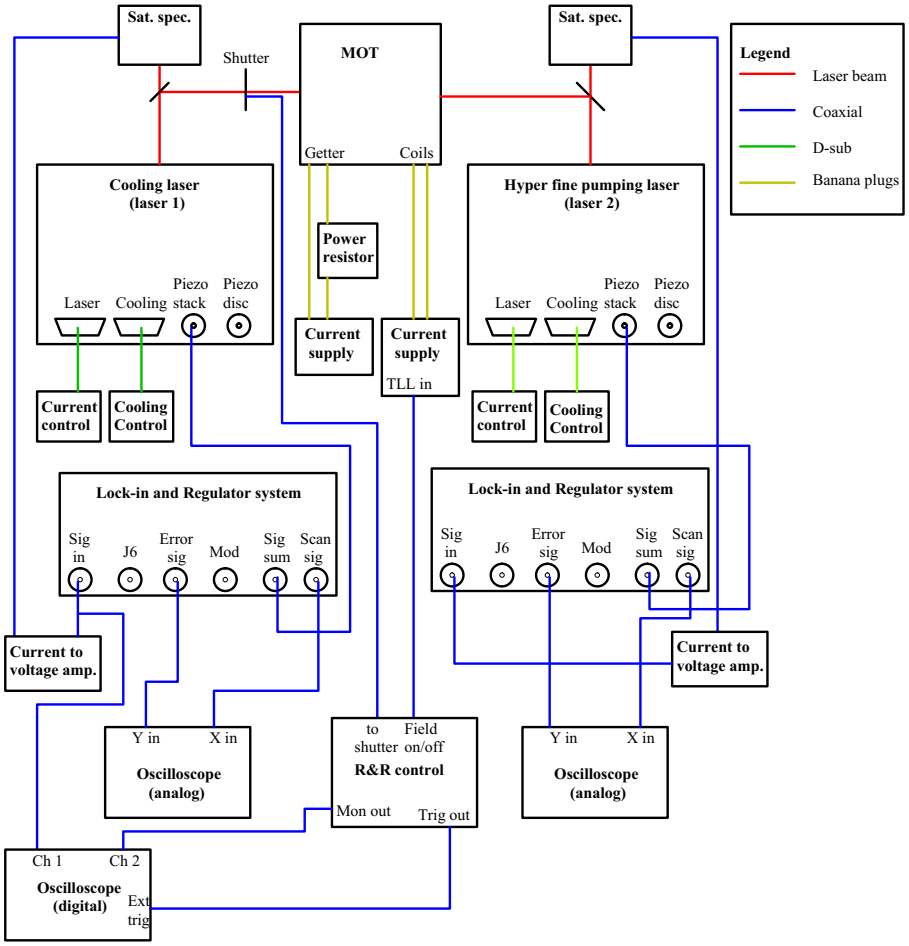

Figure 3.1: The electronical setup.

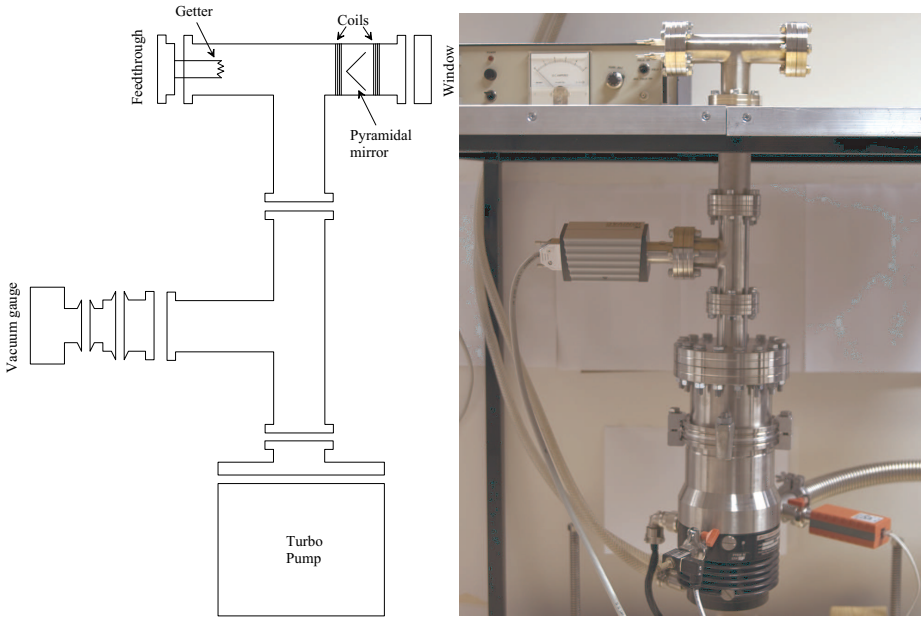

Figure 3.2: The vacuum system.

3.1.2 Pump

Our setup uses just one turbo-pump (and a pre-vacuum rotary pump). Similar setups uses an ion-pump as well [4, 6] to reach even lower background pressures. The pump is controlled via a standard turbo-pump controller from Edwards. The turbopump starts when a pre-vacuum pressure of $5{\cdot}10^{-2}$ mbar is reached.

Principle for a turbomolecular pump

The turbo-pump in the setup is a Edwards Ext 200/iso 100, dimensioned for a bigger chamber than the one used in out setup. This is needed to get rid of excess Rubidium and to maintain a stable pressure with just one pump.

The turbomolecular pump was invented in 1957 by Becker [11] and the principle design can be found in figure 3.3. It is a mechanical pump that can reach low pressures. It has fast spinning rotor ($\sim$500 m/s) that carries momentum to the gas molecules. When the pressure is sufficiently low ($<$ 10^{-3} mbar), which is when the mean free path of the molecules is longer than the distance between the rotor blades, collisions with the rotor are far more probable than collisions with a gas molecule. To reach this low pressure a turbo-pump has to backed up by a pre-vacuum pump.

Heavy molecules travel with slow speed. This means that the turbopump will be very effective to get rid of the excess Rb since the probability for back-

diffusion (see figure 3.4) will rise for the relatively heavy Rb.

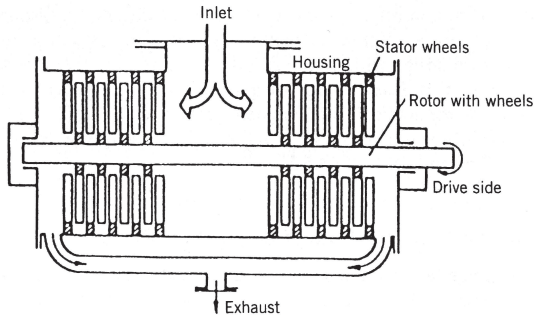

Figure 3.3: Principle design of a turbomolecular pump [11].

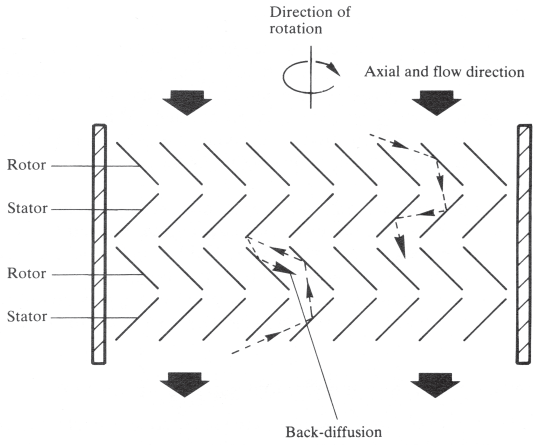

Figure 3.4: Back-diffusion in a turbomolecular pump [16].

The pre-vacuum pump allows us to pump down to 10^{-3} mbar and the turbopump reaches $4 \cdot 10^{-9}$ mbar within a few days. At first, only a pressure of a few 10^{-7} mbar was obtained. This was a disappointment, but after some work to get rid of unnecessary O-ring couplings and the use of a leak detection spectrometer[1] it was possible to reach the pressure stated above.

Since the pressure in the chamber, when everything worked as intended, was only a few 10^{-9} mbar, no bakeout was needed. If the pressure will not come down, the procedure for bakeout is described in [16, 17].

[1]We finally found that a welding in one of the ordered vacuum pipe adapters where leaking.

3.1.3 Pressure measurements

When vacuum technology started, mercury manometers were used and it is no surprise that the unit mmHg (or Torr) is still very common. It is however not permitted by the Système International (SI) whose unit for pressure is Pascal (Pa). The most common unit today is the millibar (mbar), temporarily allowed in the ISO standards, 1 mbar=0.75 Torr=100 Pa.

High pressure

To be able to determine when the turbo-pump should start, one needs to measure the pressure between the pre-vacuum pump and the turbo-pump.

A pressure gauge that works in the wanted area is the Pirani gauge. The Pirani gauge, invented by von Pirani in 1906, was a very important invention since it made the mercury-McLeod gauge unnecessary. The principle is that the temperature of a hot wire is measured from a distance. Since the transferred temperature depends on the thermal conductivity of the gas, a lower pressure gives a lower heat transfer. The temperature is measured by the change in resistivity in a second wire. In our setup, we use an Edwards active Pirani gauge able to measure in the area 10^3–10^{-4} mbar.

Low pressure

To measure the pressure in high vacuum ($<10^{-4}$ mbar) is not an easy task. The only gauges available in the stated pressure range are cold cathode and hot cathode ionization gauges.

A space containing gas between two electrodes with high voltage will be ionized. Positive ions will be attracted by the cathode and give rise to a current through the space. This current is directly related to the number of ions and consequently the number of molecules. This simple setup is limited to measure down to 10^{-7} mbar, below that the production of electrons for ionization gets too low. The solution is to include a heated filament which provides free electrons at a controlled rate via thermionic emission[2].

In our setup we use a Leybold Ionivac gauge, able to measure in the area 100–10^{-12} mbar by combining the hot cathode technique with a high pressure technique.

3.2 Rb-source

The trap has to be loaded somehow. A MOT can be loaded in two ways: from a thermal source slowed down by a counter-propagating beam, or from

[2]When heated, the freely moving atoms in the metal can come across the potential barrier.

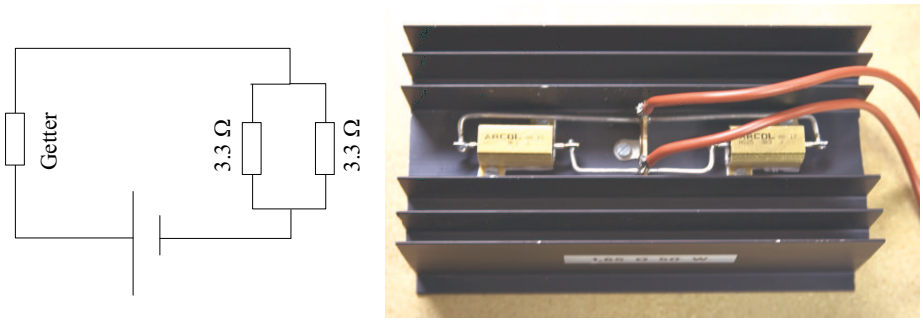

Figure 3.5: Circuit diagram and photo of the power resistor.

the slow part of a Maxwell-Boltzmann velocity distribution of the hot background vapor. The trap has to be loaded with a lot of atoms to allow the trap to fill fast, but on the other hand that will lead to a higher pressure and a shorter lifetime. The source most easy to use is a commercial "getter" for industrial application [13].

The getter releases atomic Rubidium when heated to a few hundred degrees C by applying an electric current. The stated threshold for operation is 2.7 A, but it has been found that an initial current of 8 A for 2–5 s is needed to get it started [14]. After that, the threshold is well defined at 2.7 A and an operational current of 3–4 A has been found to give an adequate flux [14]. A power resistor has to be put in series with the getter since the getter it self has almost no resistance[3]. In this thesis a resistor of 1.65 Ω 50 W, consisting of two parallel coupled 3.3 Ω resistors mounted on a cooling flange (see figure 3.5), is used. The current through the getter and the resistor are controlled by a commercial power supply.

The getter has a capacity to load the MOT with more than 10^8 atoms in just a few seconds, despite of the high temperature of the getter, and still keep the lifetime of the trap at high numbers [14]. Two getters are mounted directly on the electrical feedthrough pins with the metal parts of a small connection block (see figure 3.2). This design makes it easy to change getters and was invented by the author.

3.2.1 Capture limit

In figure 2.4 it can be seen that the friction force increases when the speed of the atoms increases, but then decreases when the Doppler shift becomes longer from the detuning. This means that atoms with large speeds will not be cooled. Atoms moving with a speed which makes them just at the boundary of absorbing light and thus slowed down are at the capture limit. [1]

[3] The low voltage makes it hard to control the current with the power supply.

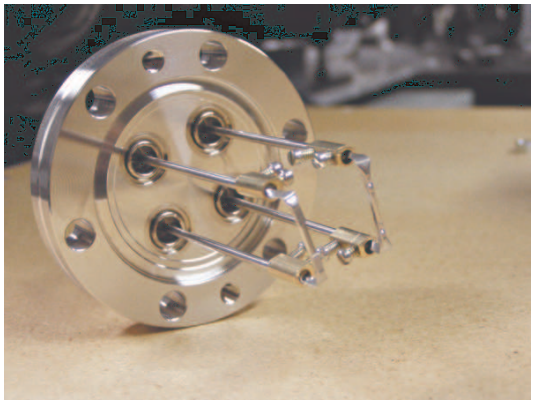

Figure 3.6: The getter mounted on the electrical feedthrough using the metal parts from a small connection block.

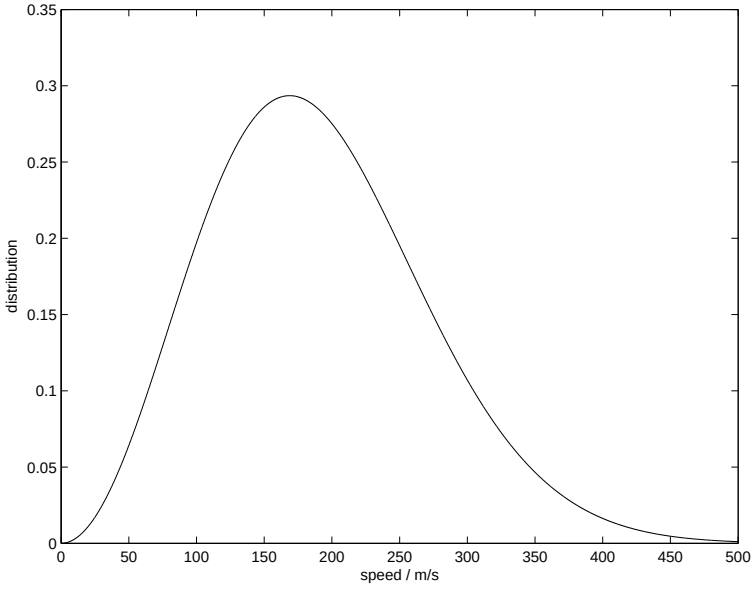

Figure 3.7: The speed distribution of rubidium atoms at T=293 °K.[1]

The capture limit is dependent on the detuning. A large detuning makes it possible to cool many atoms, but on the other hand they will not be cooled as much. The detuning that creates the coldest sample is $\delta_l = -\gamma/2$. For this detuning the capture limit is defined as [36]:

$$v_c k \equiv \gamma \tag{3.1}$$

Sometimes it is useful to express the capture limit as a temperature.

$$k_B T_c \equiv \frac{M\gamma^2}{k^2} \tag{3.2}$$

M is the atomic mass. For ^{87}Rb the capture limit is 4,6 m/s or 0,22 K.

A common way of loading a MOT is to catch atoms from the background vapor. In the design described in this report, that method will be used to load the trap with one of the Rubidium isotopes. The capture limit is approximately valid for a MOT, although there is a position dependent frequency shift in addition to the Doppler shift. There is just a tiny fraction of the atoms that move slower than the capture limit if the atoms are at thermodynamic equilibrium at room temperature. At thermodynamic equilibrium, atoms are Maxwell-Bolzmann distributed, (equation 3.3 [47]). The Maxwell-Boltzmann distribution for ^{87}Rb at room temperature is plotted in figure 3.7.

$$f(v) = \frac{4}{\sqrt{\pi}}(\frac{M}{2k_B T})^{3/2} v^2 e^{\frac{mv^2}{2k_B T}} \tag{3.3}$$

In ^{87}Rb about 15 atoms out of 100 000 move below the capture limit. The detuning can be increased in order to catch a larger fraction of the atoms.

3.3 Magnetic field

The magnetic field gradient required to trap the atoms is produced by a pair of coils in anti-Helmholtz configuration, see figure 3.8. The magnitude of the magnetic field from a single coil at a distance z from the coil is:

$$B(z) = \frac{\mu_0 I r^2}{2(r^2 + z^2)^{3/2}} \tag{3.4}$$

See figure 3.8 for an explanation of the notations.

A field gradient of 10 G/cm is required [6] and it is obtained in the setup. For our setup we calculated the coils to have a diameter of 44 mm with a distance[4] of 22 mm, wound out of 16 turns 0.8 mm insulated copper wire outside a piece of plastic tubing, allowing it to slip in the z-direction. A current of 4 A gives a field gradient of 11 G/cm and heats the coils by 1.5 W. The form of the resulting magnetic field can be found in figure 3.9.

[4]The distance should be equal to the radius for maximum trapping force.[6]

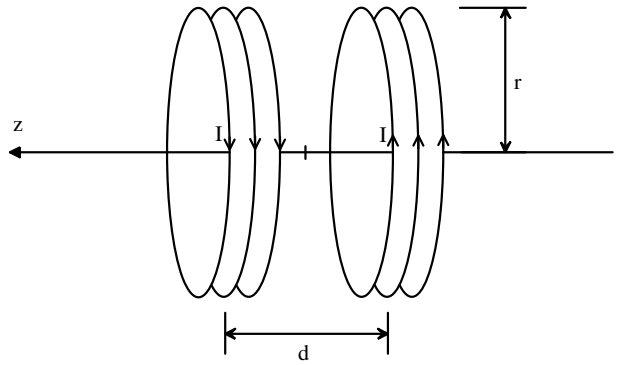

Figure 3.8: Two coils in anti-Helmholtz configuration

To get an insulating distance between the coils and the vacuum system, a piece of plastic tubing were manufactured by the workshop fo fit outside the ConFlat flange.

3.4 Pyramidal mirror

A pyramidal MOT (figure 3.10b) has many advantages compared to the traditional design (figure 3.10a). It is reliable, easy to setup and use and it reduces the optical components needed to a minimum (e.g. one quarter-wave plate instead of six). The three pairs of circularly polarized beam are automatically created inside the MOT by letting an expanded circularly polarized beam getting reflected inside the pyramid.

The pyramidal mirror is manufactured out of four coated glass pieces (see figure 3.11) and is mounted in a stainless cone, manufactured from a block of stainless steel (see figure 3.12) using small amounts of low vapor epoxy[5]. The design is very similar to [4] with small modifications to increase the diffusion of Rb into the pyramidal mirror.

The glass pieces are coated with silver. Gold has a higher reflectivity at 780 nm, but it tends to attract Rb. A dielectric coating would give higher reflectivity but is likely to change polarization. A dielectric coating that addresses this issue has been developed by Arlt [37] but is too complicated for this setup. With silver, a reflectivity of 97% and a polarization contamination of 2.5% per reflection has been reported [4], which is well within the aim of this project.

A French company cut and coated the glass pieces, but they made mistakes in reading the blueprints (figure 3.11), resulting in long delays for the project.

[5]The epoxy used is Torr Seal low vapor pressure epoxy, available from Varian Inc., normally used as sealant for high vacuum applications.

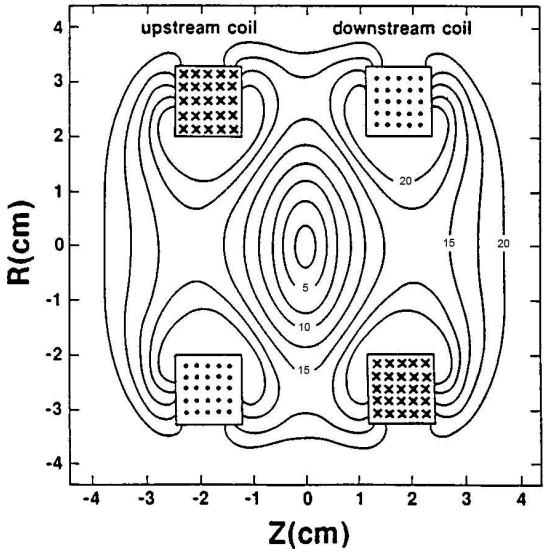

Figure 3.9: The magnetic field from a pair of coils in anti-Helmholtz configuration.

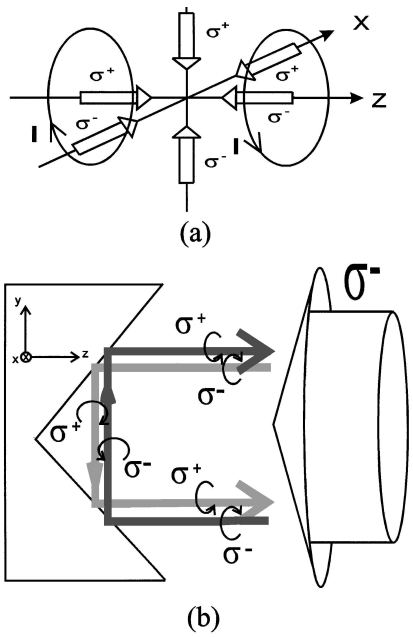

Figure 3.10: (a) The circularly polarized beams and the coils of a conventional MOT. (b) The partial beams of a pyramidal MOT.[38]

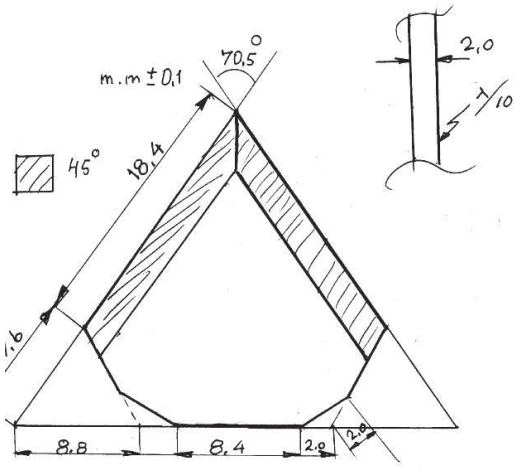

Figure 3.11: The four identical glass pieces that forms the pyramidal mirror. Measurements in mm.

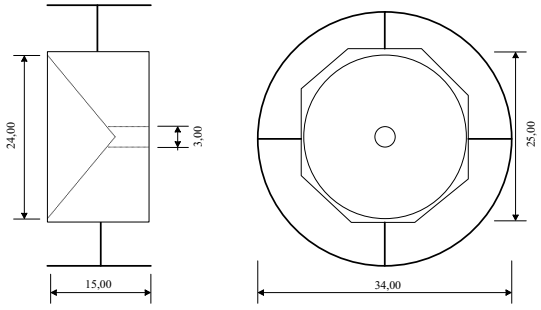

Figure 3.12: The pyramidal mirror mounting block in stainless steel. The machined cone has an angle of 109°.

3.5 Observation system

To align the setup, a transmissive IR-card and an IR-viewer are very helpful. To make the measurements on the trap, one needs a photo diode and a simple current-to-voltage amplifier. An IR-sensitive CCD-camera would be a great help to get the trap running and to perform measurements of the size of the captured cloud.

3.6 System for release and recapture

The release and recapture (R&R) system is chosen for simplicity. One needs fewer optical components, and since the optical access in the pyramidal setup is limited there is not enough room to send in a probe beam. The time-of-flight method gives more accurate measurements, but the 10% error [15] estimated by the R&R-technique is acceptable for the purpose of this MOT.

To implement the R&R-method, one needs to be able to shut off the the laser and magnetic field. The timing between these and the measurement is critical and needs to be adjustable. The trapping laser is blocked by an electromagnetic relay and the magnetic field is cut off by a TLL-pulse to the current supply. After a short period of time ($\sim$10-100 ms, the release time) the laser and the magnetic field are turned on, and after 50 ms a measurement of the fluorescence is performed with a photodiode. The measurements of different release times yield a differentiated Maxwell-Boltzmann distribution, and hence the temperature can be calculated. A block schematics of the controller can be found in figure 3.14. The principal design is by the author and was implemented by the electronics workshop. It has not been tested in the setup yet.

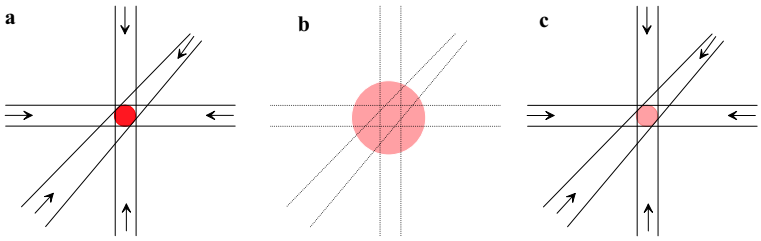

Figure 3.13: Release-and-recapture method for temperature measurement. The time from **a** to **c** is the release time, 10-100 ms.[22]

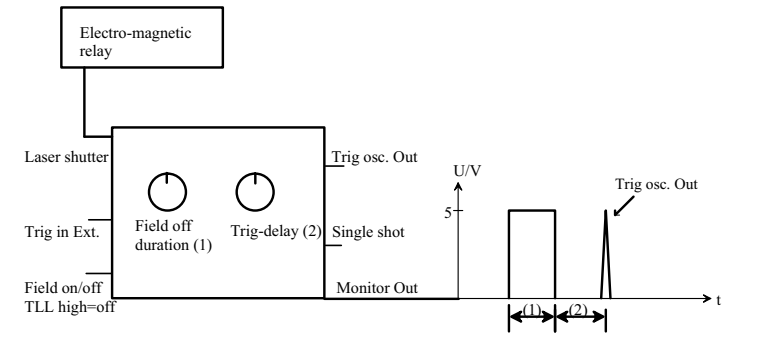

Figure 3.14: Principle design and photo of the R&R control.

Chapter 4

The optical setup

The experimental setup is installed on an optical table in the picosecond laboratory of Lund High Power Laser Facility.

4.1 General description

The setup is by no means optimized for performance, but since the output power from the lasers is so good, there is no need for anything fancier.

Two external cavity diode lasers are frequency locked in a saturation spectroscopy setup. A Burleigh wavemeter is used to assist in the frequency adjustment of the lasers. The rest of the light is then expanded, shaped and made circularly polarized before it hits the window of the chamber.

The layout of optical components on the optical table can be seen in figure 4.1.

4.2 Lasers

The lasers in the setup are two external cavity diode lasers (ECDL), designed and built by Erik Gustafsson [1]. The design mostly follows [5, 42], using high power laser diodes mounted in a Littrow configuration external cavity. In our configuration, 20% of the laser light is reflected back to the diode, increasing the cavity length. This gives the laser a smaller bandwidth and allows us to easily tune the laser frequency.

Here, we give a small summary of the laser design, characteristics and operations. For a detailed discussion of the design and the construction of the ECDL's, see [1].

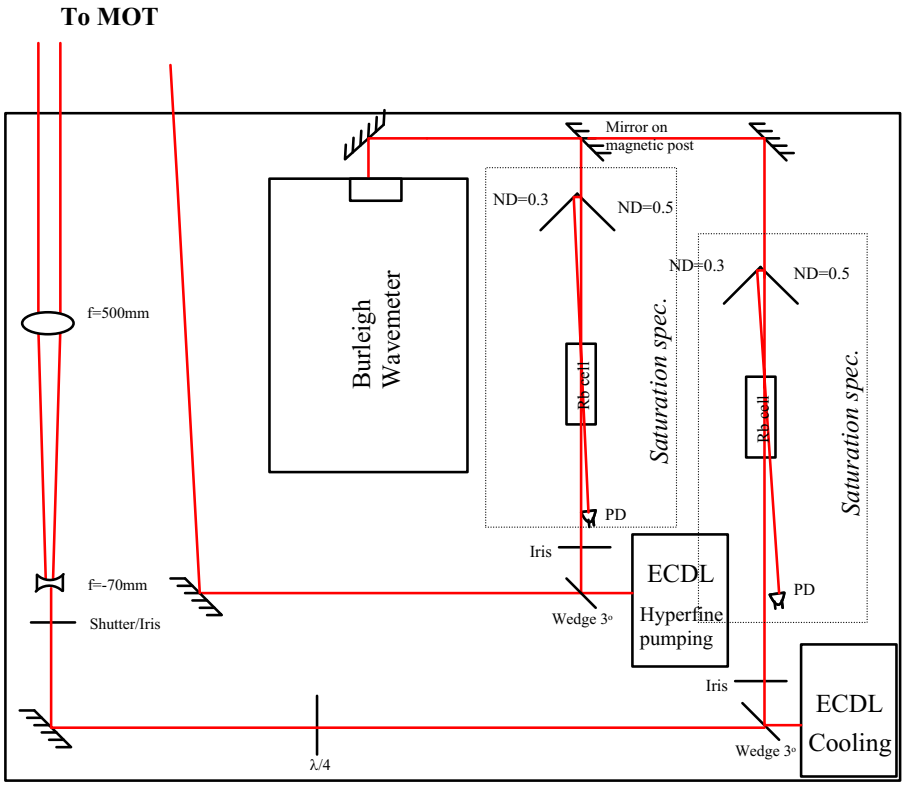

Figure 4.1: The layout on the optical table, it measures 120x90 cm.

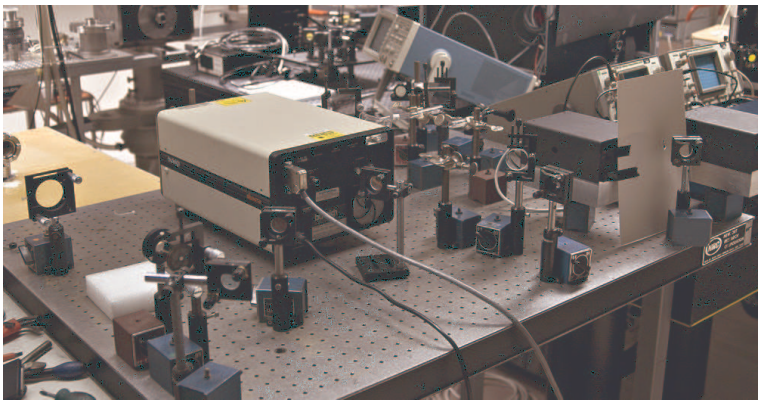

Figure 4.2: A photo of the optical setup in the picosecond lab of Lund High Power Laser Facility.

4.2.1 Laser diode

We use laser diodes from Sanyo[1] which have a high power output in the desired wavelength region.

In high power laser diodes, the back surface is often reflection coated, and the front surface is anti reflection coated. The gain in the active layer is higher than in low power diodes. The obtained linewidth is not very different from a diode with two uncoated ends. The diode that was used in the constructed system is a high power diode, rated to deliver 80 mW.

The beam that leaves the laser diode is divergent. The laser beam therefore has to be collimated[2]. The divergence of the used diode is $\theta_{\perp} = 17°$ and $\theta_{//} = 7°$. $\perp$ denotes the divergence perpendicular to the polarization direction and // parallel to the polarization.

4.2.2 Grating feedback

To make the diode laser more tunable without mode jumps and to narrow the emission linewidth of the laser, external cavities with frequency selective feedback are often used. External cavity diode lasers are also more stable and suitable to lock at a precise frequency. In this project a Littrow designed external cavity was used for this purpose.

In a Littrow configuration the minus first order is coupled back to the diode laser by a grating (figure 4.3). The normal grating equation applies:

$$d \sin \alpha = \frac{\lambda}{2}$$

In our case with d=1800 lines/mm[3] and $\lambda = 780$ nm we have a grating angle α of 44.6°.

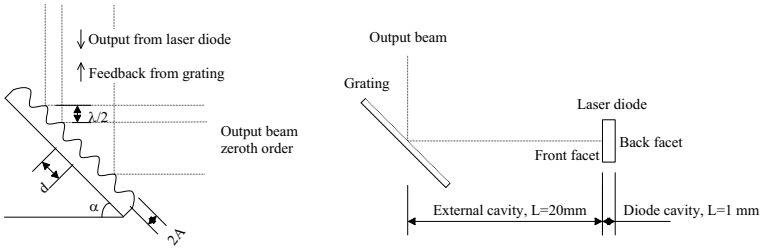

Figure 4.3: The principal design of an external cavity diode laser (ECDL).

The increased cavity length compared to the diode, combined with a good mechanical stability of the mirror mount, reduces the linewidth considerably.

[1] Single mode diode laser, part nbr. DL-7140-201.

[2] We use a collimating lens from Thorlabs, part nbr. C230TM-B

[3] We use gold coated gratings from Richardson Grating Laboratory, part nbr. 33999FL02-330H.

A linewidth of 370 kHz has been reported on the type of laser that has been constructed [42]. This narrow linewidth implies high quality current and temperature controllers.

No matter what type of laser, it always tends to lase where the losses are as small as possible. When trying to control the frequency of a diode laser by placing it in an external cavity with frequency selective feedback, the lowest losses must be at the desired frequency.

If the front facet of the diode laser is antireflection coated, a cavity is created between the back facet of the diode laser and the grating, see figure 4.3. To get laser action the losses must be smaller than the gain. The gain profile can be moved by changing the temperature of the diode to place the center of the gain profile closer to the desired lasing wavelength. The angle of the grating selects one of the cavity modes where the laser will lase.

The laser used in this design has a partly antireflection coated front facet. The cavity of the diode is still present and a compound cavity is formed. To minimize the losses at the frequency of the external cavity mode selected by the grating, two conditions have to be fulfilled. The gain curve has to be moved to place its center close to the desired lasing wavelength. In addition to that, one of the diode cavity modes has to be placed at the frequency of the external cavity mode that is selected by the grating. If this is not done, the losses might be smaller when the diode is lasing in the short cavity mode that is in the center of the gain profile.

4.2.3 Design

The ECDL's are constructed on a modified Newport mirror mount with fine adjustment screws. Figure 4.4 shows the modified frontplate of the mirror mount. The grating is mounted on a grating holder (see figure 4.5), fixed on the frontplate by screws. The fine adjustment screws allow to change the output frequency by changing the grating angle. To allow even finer tuning, a piezo disk and a piezo stack are added (see figure 4.6).

The mirror mount is fixed on an aluminium base plate where a temperature transducer[4] is mounted. This is the temperature feedback to the temperature controller. A Peltier element[5] is mounted between the base plate and a big aluminium block that acts as a heat sink.

4.2.4 Tuning

There are several ways to tune the wavelength of the lasers. The goal is to have a strong florescent signal in the Rb-cells, seen through an IR-viewer. If the signal is weak (i.e barely visible), the laser probably lases in the wrong cavity and this can be solved by a small change of the current to the laser.

[4] AD590.

[5] From Supercool, cooling power 20 W at 9.2 V and 3.9 A.

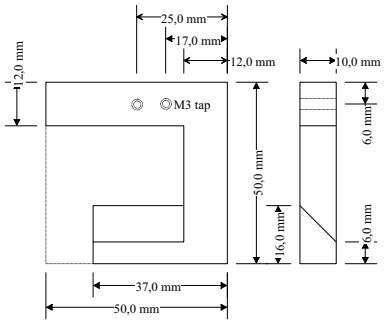

Figure 4.4: Drawing of the modified frontplate.[1]

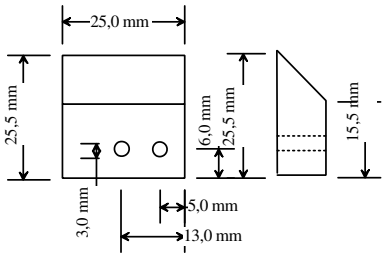

Figure 4.5: Drawing of the grating holder.[1]

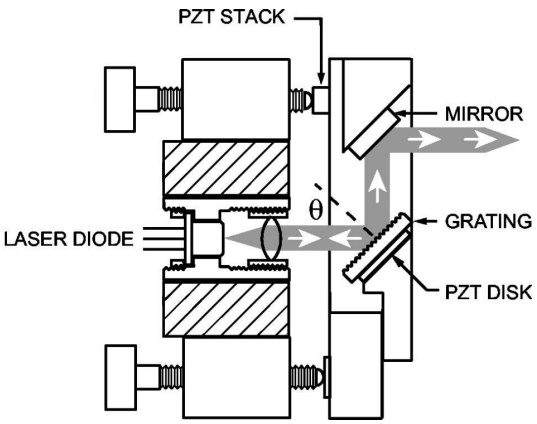

Figure 4.6: A cross section of the external cavity diode laser. [42]

A wavemeter is of great use here, at least the first times the tuning is performed. The resolution does not have to be better than ±0.1 nm, do not forget to check if it is the vacuum or air wavelength that is shown (the author has bitter experience of this).

A summary of the tuning parameters can be found in table 4.1.

Grating angle	1.2 nm/rev
Piezo stack	1 GHz/5V
Piezo disk	0.1 GHz/5V
Temperature	0.25 nm/°K
Current	1 GHz/1mA

Table 4.1: The tuning parameters of the laser.

Grating angle

The initial alignment of the grating should be such that the reflected beams goes right back in the diode. With an IR-card, one can observe one strong and one weak dot, the later origins from the surface of the collimating lens. These two dots should overlap.

A procedure for precise vertical alignment of the minus first order return beam is described in [3]. Reduce the current through the diode to just above threshold[6] and adjust the angle of the grating around a horizontal axis until there is a significant rise in laser output power. After this, the threshold current should be lower than before, since the laser now gets light coupled back to the internal cavity.

The horizontal alignment should be such the angle equals the Littrow angle of 44.6°. If the grating is misaligned, the output wavelength is insensitive to small changes around the vertical axis, or it will only move a small amount and then jump backwards [3]. After this, the vertical alignment should be checked once more.

Small changes to the grating angle around the vertical axis now changes the frequency of the reflected light. This is controlled partly by a fine adjustment screw (25 μm/rev), partly by a piezo-electric stack. The latter can perform a 1 GHz scan at $\Delta V = 5$ V without mode jumps. This means that very simple electronics can be used to perform a frequency scan.

Cavity length

Behind the grating there is a piezo disc to change the cavity length. At $\Delta V = 5$ V, it changes the frequency with 0.1 GHz. It has not been used for

[6] In our case 30 mA.

any practical purposes yet, since it would need a high-voltage amplifier to scan over the desired line.

Temperature

In free run at 25°C, the diodes emit light at 783 nm. With changing temperature the change in the gain profile is greater than the change in the cavity modes of the laser. Since a laser always lases where the smallest losses are, the wavelength changes about 0.06 nm/°K. If one includes the mode jumps, the average displacement is 0.25 nm/°K [3]. This means that one has to cool the lasers to about 15°C, a temperature where condensation of water becomes a problem. The dew point depends on the temperature and relative humidity. The lab is temperature-controlled to 21°C and some calculations (see figure 4.7) gives that the humidity has to be over 65 % to give a dewpoint at 14°C. This presents a problem during the summer when the air have to be cooled. Condensation has been observed during September and October and the lasers have to be covered to minimize the volume of air than can condensate.

Temperature gradients when changing the temperature are also a big problem. The system needs about one hour to become stable enough for initial wavelength tuning.

The temperatures are controlled via two commercial temperature control units from Melles Griot (06 DTC 101 TEC Controller). The long term temperature drift is less than 0.001°K per hour. The gain should be lowest possible to avoid oscillations since the mass of the controlled system is large.

Drive current

The currents to the lasers are controlled by two commercial power supplies from Melles Griot, the cooling laser is controlled by a series 200, and the repumping laser is controlled by a 06DLD201. The laser diodes have an operating current of maximum 140 mA and the drivers should be limited to not give any higher current.

While tuning the lasers with the drive current, note that the lasers exhibit hysteresis and that changing the current back to the old value does not mean that the laser is at the old wavelength.

4.2.5 Stabilization

To be able to cool atoms and to perform experiments on them, the laser has to be locked to a certain frequency. This is mostly to reduce the short term variations, such as mechanical vibrations, electronical fluctuations and even variations in atmospheric pressure caused by draft and talking. The long term variations of about 20 MHz/h are not a big concern and can be corrected by hand.

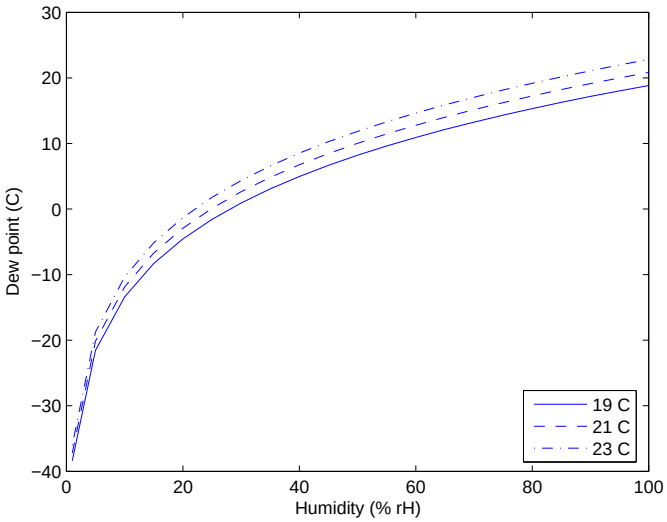

Figure 4.7: The dew point as a function of temperature and relative humidity. The calculations are performed by the author following [28].

In our setup, we use an advanced design with an integrated lock-in amplifier/PI-regulator, which is also used by Anders Kastberg's group in Umeå. A photo can be found in figure 4.8. Still there are some problems with this system, the error signal does not appear, and the lasers have not been locked yet.

Figure 4.8: The lock-in/PI-regulator used in our setup.

Frequency modulation

The frequency of the laser light is shifted by a sinusoidal signal to the piezo stack, and a reference of this signal is sent to the lock-in circuits. The amplitude should be so large that it shifts the light with around 30 MHz with a frequency of at least 1 kHz.

Lock-in amplification

The modulated laser light seen by the photodiode is then mixed with the internal reference signal. Here, of course, the phase has to be adjusted since there will be a delay before the photodiode registers the change. The two signals are multiplied, giving a two term product, consisting of the total frequency and the difference in frequency, in this case as a DC-level. A low-pass filter takes away the total frequency term, leaving only the difference in frequency. This signal is equivalent to the derivative of the signal. This will turn a hyperfine peak into a steep ramp, ideal to lock on.

Feedback

If the modulation is small enough, so that only a small, approximately linear, portion of the Lorentzian peak is scanned, the derivative produced in the lock-in circuits will be a positive, negative or zero DC signal. After amplification (called gain), the signal is sent to the piezo stack, changing the output frequency until the error signal reaches zero.

Four different signals can be sent from the lock-in/PI-regulator unit to the piezo stack. Besides from the modulation and error signal described above, a saw tooth and a DC-level can be applied as well. These are used to "zoom" into the peak of interest.

Practical use of the system

This is the workflow for our system to obtain a frequency locked laser:

1. Change "Amp" and "Offset" so that the laser sweeps over one or a few peaks. Turn modulation on. Change "Phase" until the error signal gets maximized.

2. Change "Lock offset" until the point on the peak one wishes to lock hits 0 V.

3. Change "Scan" from "Auto" to "Man". Change "Scan sign." until one hits the correct point on the peak.

4. Turn "Lock" "on". There is 50% chance that the sign on the locking is correct. If the signal travels the wrong way, change phase by 180°.

4.3 Saturation spectroscopy

Saturation spectroscopy is a really exciting phenomena for undergraduate exercises and can be used as a stand-alone experiment. Sub-doppler spectroscopy using two counter propagating beams with pump-probe geometry is

an excellent introduction to non-linear spectroscopy. The basics of saturated absorption spectroscopy are discussed in several textbooks [18, 44].

In our setup, we use the Doppler free hyperfine peak to lock the lasers to a precise frequency.

4.3.1 The basics

The principle of saturation spectroscopy is that the probe beam monitors the change of absorption, which comes from the medium's interaction with the pump beam. As described in section 2.2.1, for a two-level system, the steady state population difference $\Delta N = (N_g - N_e)$ can be expressed as [19]

$$\Delta N(\omega_L, v_z) = \Delta N^0(v_z)(1 - \frac{I/I_s}{1 + I/I_s + (2\delta/\gamma)^2})$$

In the limit where the incident light is very bright ($I_s \ll I$), the population difference goes towards zero. The line shape becomes a power broadened Lorenzian in which spectral hole-burning occurs. This yields a spectra like the one i figure 4.9(a).

4.3.2 Crossover resonances

As one can see in figure 4.9, the spectra has twice as many peaks as expected. Each of this six peaks occurs when the pump and the probe simultaneously excites the same velocity class or classes. The three peaks explained by the basic theory occur when the pump and the probe both excite atoms with zero velocity. The other three peaks, the crossover resonances, occur when the laser has a frequency exactly between two transitions.

When out of resonance, the pump and probe does not favor any velocity class, but at the crossover frequencies the pump and probe both excite two classes[7]. This results in that the probe sees a decrease in the number of atoms in the ground state, giving rise to hole burned in the velocity distribution.

4.3.3 Saturation spectroscopy setup

A small portion of the light (4%) is split off by a simple wedge, oriented in such a way that the transmitted and one of the reflected beams are parallel to the optical table. An iris eliminates the second reflected beam. The smaller beam enters the saturation spectroscopy setup. It travels through a ^{87}Rb-cell and is retro-reflected back by two reflective neutral density filters. This gives a probe beam power of 15% compared to the pump beam. The light transmitted through the ND-filters can be lead into a wavemeter.

[7] For a given frequency blue shifted atoms moving in one direction and red shifted atoms moving in the other direction get excited to their respective exited state by the same beam at the same time.

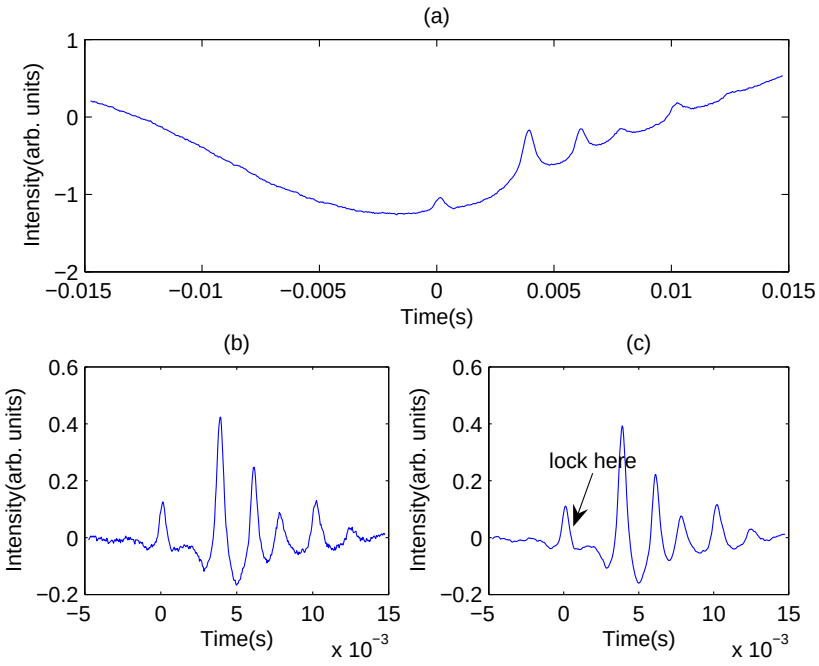

Figure 4.9: **(a)** A saturation spectra obtained from the experimental setup for ^{87}Rb ($F = 2 \rightarrow F'$) with increasing wavelength to the right. This is the signal straight from the photo diode without lock-in amplification. The peaks from left to right: F= 2 →F'= 3, a crossover resonance (F= 2 →F= 2, 3), F= 2 →F'= 2, a cross over resonance(F= 2 →F'= 1, 3), a crossover resonance(F= 2 →F'= 1, 2) and F= 2 →F'= 1. **(b)** The same spectra normalized via a high-pass filter. **(c)** The spectra filtered through a low-pass filter

The pump-probe beams should overlap as much as possible to give a good signal. A piece of cardboard, black on one side and white on the other, with a small hole, placed in front of the RB-cell makes it easier to align the weak probe beam. The probe beam then hits a standard photodiode connected to a simple commercial current-to-voltage amplifier.

Since there is pure ^{87}Rb in our cells, only two Doppler broadened structures emerge (if it was atomic rubidium, the isotope shift of ^{85}Rb would give rise to two more structures). These are separated by about 7 GHz due to the ground state hyperfine splitting. The structure with the highest wavelength is used for cooling, and the one with lowest is used for repumping.

Within the sub-Doppler spectra it is easy to identify the correct hyperfine transition. It is always the peak which is a little bit on its own, clearly visible to the very left in figure 4.9. The laser should be locked on the right side (towards the other transitions) to give the desired detuning.

4.4 Beam shaping, expansion and polarization

4.4.1 Cooling optics

The laser beam locked to the cooling transition has to be shaped, expanded and given the necessary circular polarization. This is achieved with a quarter-wavelength plate ($\lambda/4$-plate). The laser light is linearly polarized so a $\lambda/4$-plate, with an optical axis oriented 45° respective to the polarization, will create circularly polarized light.

To expand the beam to cover the pyramidal mirror area, a simple telescope is used. Two lenses with focal lengths f=-70mm and f=500mm, with a distance of 430mm, will expand the beam to the desired size. The result will however be quite elliptical due to the geometry of the laser beam. An iris in front of the telescope will make the beam more circular in geometry, but throws a lot of light away. An anamorfic prims pair would shape the beam without the big losses, but was too expensive for this setup.

4.4.2 Repumping optics

The repumping laser does not need any extra optics for shaping, expansion or polarization, but the beam can be too strong, requiring some way to reduce the laser power (e.g polarizer or ND-filter).

Chapter 5

Conclusions

The aim of this thesis was quite clear: to build and test the MOT. The last part has not yet been realized. The frequency locking is still not working but all the parts are present and we are very close to obtaining a working MOT.

Besides the frequency locking problem, there was a big delay in getting the pyramidal mirror, only the third time did the company follow the blueprints. The construction of the vacuum system also took a long time. Eventually a leak detector spectrometer had to be used to find a leaking important weld.

Working alone and without the support that a laser cooling group in Lund would be able to give, has been very challenging.

The design has been changed a few times to keep the low cost constraint. Erik Gustafsson used around 25 000 SEK, and I used around 35 000 SEK, giving a total cost of 60 000 SEK. Compared to the amount of physics available to teach in the laboratory this is a bargain. Hopefully this will interest students in the rapidly expanding field of cold atoms, and atomic physisc in general.c

Acknowledgements

The author would like to thank the following persons, without whose assistance this project should not have been possible,

My supervisor Anne L'Huillier, who as my lecturer in *Laser Physics* and *Atomic Physics, Advanced Course*, really arouses enthusiasm in the subject,

Erik Gustafsson, who started this project,

Anders Kastberg and his group in Umeå, especially Robert Saers and Peder Sjölund, for all help and a very rewarding visit,

Ingela Roos for accommodation during my stay in Umeå,

Åke Bergquist for helping me realize my ideas into electronical circuits,

Lars Rippe for listening to and trying to answer my endless questions,

Per Jonsson for help with the vacuum system,

and Victoria Olsson for help with language check.

Bibliography

[1] E. Gustafsson, *Design study of a Magneto-Optical Trap for laser cooling of rubidium atoms*, Lund Reports on Atomic Physics LRAP-325 (2004)

[2] O. Svelto, *Principles of lasers*, Kluwer Academic/Plenum Publishers (1998)

[3] K.B. MacAdam *et al*, *A narrow-band tunable diode laser system with grating feedback, and a saturated absorption spectrometer for Cs and Rb*, Am. J. Phys. **60**, 1098-1111 (1992)

[4] C. Wieman and G. Flowers, *Inexpensive laser cooling and trapping experiment for undergraduate laboratories*, Am. J. Phys. **63**, 317-330 (1995)

[5] A. S. Arnold, *A simple extended-cavity diode laser*, Review of Scientific Instruments **69**, 1236-1239 (1998)

[6] A. Mellish, A. Wilson, *A simple laser cooling and trapping apparatus for undergraduate laboratories*, Am. J. Phys. **70**, 965-971 (2002)

[7] A.A. Radzig and B.M Smirnow, *Reference data on Atoms, Molecules and Ions*, Springer series in Chemical Physics **31**, Springer (1985)

[8] S. Bize *et al*, *High accuracy measurement of the* ^{87}*Rb ground-state hyperfine splitting in an atomic fountain*, Europhys. Lett. **45**, 558-564 (1999)

[9] D.A. Steck, *Rubidium 87 D Line Data*, Los Alamos National Laboratry, availible from http://steck.us/alkalidata (2003)

[10] Stony Brook State University of New York, Department of Physics & Astronomy, availible from http://felix.physics.sunysb.edu/PAM/highlights/molasses.html, accessed 23 of March 2005

[11] W. Becker, Vak.-Tech. **7 5**, 149-152 (1958)

[12] M. Greiner, *Ultracold quantum gases in three-dimensional optical lattice potentials*, Ludwig-Maximilias-Universität, Munich (2003)

[13] SAES Getters S.p.A., www.saesgetters.com, Order nr. RB/NF/3.4/12 FT10+10

[14] U.D. Rapol, A. Wasan, V. Natarajan, *Loading of a magneto-optic trap from a getter source*, Indian Institute of Science, India (2001)

[15] Shih-Kuang Tung *et al*, *Cooling Atoms Below 100 μK*, Chinese journal of physics **38**, 395-399 (2000)

[16] Nigel S. Harris, *Modern Vacuum Practice*, McGraw-Hill (1989)

[17] J.M Lafferty (ed.), *Foundations of Vacuum Science and Technology*, John Wiley & Sons (1998)

[18] M.D. Levenson and S.S. Kano, *Introduction to Nonlinear Laser Spectroscopy*, Academic (1988)

[19] W. Demtroder, *Laser spectroscopy*, Springer (1998)

[20] V.S. Letokhov, *Cooling and capture of atoms and molecules by a resonant light field*, Sov. Phys. **45**, 698 (1977)

[21] T.L. Hill, *An intruduction to Statistical Thermo-dynamics*, Barnes&Noble (1987)

[22] W.D. Phillips, *Nobel Lecture: laser cooling and trapping of neutral atoms*, Rev. Mod. Phys. **70**, 721-741 (1998)

[23] E. A. Cornell and C. E. Wieman, *Nobel Lecture: Bose-Einstein condensation in a dilute gas, the first 70 years and some recent experiments*, Rev. Mod. Phys. **74**, 875-893 (2002)

[24] W.D. Phillips *et al*, *laser cooling and electromagnetic trapping of neutral atoms*, J. Opt. Soc. Am. B **2**, 1751 (1985)

[25] S. Chu *et al*, , Phys. Rev. Lett. **55**, 48 (1985)

[26] S. Stenholm, *The semi-classical theory of laser cooling*, Rev. Mod. Phys **58**, 699 (1986)

[27] F. Reif, *Fundamentals of Statistical and Thermal Physics*, McGraw-Hill (1965)

[28] J.L. Monteith and M.H. Unsworth, *Principles of Enviromental Physics*, Arnold (1990)

[29] P.D. Lett *et al*, *Optical molasses*, J. Opt. Soc. Am. B **6**, 2084 (1989)

[30] P.D. Lett *et al*, *Obervation of atoms laser cooled below the doppler limit*, Phys. rev Lett. **61**, 169 (1988)

[31] J. Dalibard and C. Cohen-Tannoudji, *laser cooling below the doppler limit by polarization gradients–simple theoretical models*, J. Opt. Soc. Am. B **6**, 2023-2045 (1989)

[32] P.J. Ungar *et al*, *Optical molasses and multilevel atoms–theory*, J. Opt. Soc. Am. B **6**, 2058-2071 (1989)

[33] Wikipedia–the free encyclopedia, availble from http://www.wikipedia.org, accessed 1 of February 2005

[34] *laser cooling and Trapping*, Experimental exercise instruction, Advanced Optics Laboratory, Colorado University

[35] X. Du *et al*, *An atom trap system for practical 81Kr dating*, Rev. Sci. Instrum. **75**, 3224-3232 (2004)

[36] H.J. Metcalf and P. van der Straten, *laser cooling and Trapping*, Springer (1999)

[37] J.J. Arlt *et al*, *A pyramidal magneto-optical trap as a source of slow atoms*, Opt. Commun. **157**, 303-309 (1998)

[38] K. I. Lee, J. A. Kim, H. R. Noh and W. Jhe, *Single-beam atom trap in a pyramidal and conical hollow mirror*, Optical Letters 21, 1177-1179, 1996.

[39] G. Grossman,*Semiconductor Physics*, Lund Institute of Technology (2003)

[40] W. W. Chow *et al*, *Semiconductor-Laser Physics*, Springer (1994)

[41] L. Engström, *Atomfysik F3 2002*, KFS i Lund AB (2002)

[42] C. J. Hawthorn *et al*, *Littrow configuration tunable external cavity diode laser with fixed direction output beam*, Rev. Sci. Instrum. **69** (2001)

[43] T. Nayuki *et al*, *Continuous Wavelength Sweep of External Cavity 630 nm Laser Diode without Antireflection Coating on Output Facet*, Opt. Rev. **5**, 267-270 (1998)

[44] S. Svanberg, *Atomic and Molecular Spectroscopy*, Springer (2001)

[45] J. J. Maki *et al*, *Stabilized diode-laser system with grating feedback and frequency-offset locking*, Opt. Comm. **102**, 251-256 (1993)

[46] G. Genty *et al*, *Analysis of the Linewidth of a Grating-feedback GaAlAs Laser*, IEEE Journal of Quantum Electronics **36**, 1193-1198 (2000)

[47] P. A. Tipler, *Physics for Scientists and Engineers*,W. H. Freeman and Company (1999)

[48] C. H. Henry, *Theory of the Linewidth of Semiconductor Lasers*, IEEE Journal of Quantum Electronics 18, 259-264, 1982.